

Report Date: April 1, 2002

Semi-Annual Report

**INVESTIGATION OF EFFICIENCY IMPROVEMENTS DURING CO<sub>2</sub>  
INJECTION IN HYDRAULICALLY AND NATURALLY FRACTURED  
RESERVOIRS**

DOE Contract No.: DE-FC26-01BC15361

Harold Vance Department of Petroleum Engineering  
Texas A& M University  
3116 TAMU  
College Station, TX 77843-3116  
(979) 845-2241

Contract Date: September 1, 2001  
Anticipated Completion Date: September 1, 2003

Principal Investigator: David S. Schechter  
Harold Vance Department of Petroleum  
Engineering

Contracting Officer's Representative: Dan Ferguson  
National Petroleum Technology Office

Report Period: Oct 1, 2001- March 31, 2002

US/DOE Patent Clearance is not required prior to the publication of this document.

## **DISCLAIMER**

This report was prepared as an account of work sponsored by an agency of the United States Government. Neither the United States Government nor any agency thereof, nor any their employees, makes any warranty, express or implied, or assumes any legal liability or responsibility for the accuracy, completeness, or usefulness of any information, apparatus, product, or process disclosed, or represents that its use would not infringe privately owned rights. Reference herein to any specific commercial product, process, or service by trade name, trademark, manufacturer, or otherwise does not necessarily constitute or imply its endorsement, recommendation, or favoring by the United States Government or any agency thereof. The views and opinions of authors expressed herein do not necessarily state or reflect those of the United States Government or any agency thereof.

## TABLE OF CONTENTS

DISCLAIMER .....	ii
TABLE OF CONTENTS.....	iii
LIST OF TABLES .....	iv
LIST OF FIGURES .....	v
Effect of Overburden Pressure on Unfractured and Fractured Permeability Cores.....	1
Experimental Work.....	1
Data Analysis .....	2
Artificially Fractured Core Simulation .....	2
Results and Discussion .....	4
Conclusions.....	6
References .....	6
Nomenclatures .....	6
Appendix-A.....	7

## LIST OF TABLES

Table 1	Overburden experiments for unfractured core.....	9
Table 2	Overburden experiments for fractured core.....	9

## LIST OF FIGURES

Fig. 1	Schematic diagram of the two-phase core flooding experiment.....	10
Fig. 2	Comparison permeability reduction between unfractured and fractured cores due to increasing overburden pressure.....	11
Fig. 3	Relationship between pressure drop and permeability .....	11
Fig. 4	Water saturation change at matrix and fracture at transient flow condition .....	12
Fig. 5	The simulation results of flow rates and pressure drop injected at 5 cc/min and overburden pressure of 500 psi .....	12
Fig. 6	The flow rates comparison between laboratory and simulation results at 5 cc/min and each different overburden pressures.....	13
Fig. 7	The pressure drop comparison between laboratory and simulation results at 5 cc/min and each different overburden pressures.....	13
Fig. 8	Effect of injection rates on matrix permeability during applying variable overburden pressures. ....	14
Fig. 9	Effect of injection rates on fracture aperture during applying variable overburden pressures. ....	14
Fig. 10	Effect of injection rates on fracture permeability during applying variable overburden pressure. ....	15
Fig. 11	Reduction in fracture flow rate during variable overburden pressures.....	15
Fig. 12	Reduction in matrix flow rate during variable overburden pressures.....	16

# **Effect of Overburden Pressure on Unfractured and Fractured Permeability Cores**

## **Introduction**

For many years many efforts have been performed in the laboratory experiments to duplicate the reservoir conditions. In this study, we will investigate the permeability change at different overburden conditions. The reduction in permeability with overburden pressure has been well known. Fatt and Davis (1952) presented the changes in permeability with pressure at range 0 to 15,000 psig and found that overburden pressure caused a reduction in permeability of the consolidated oil-bearing sandstone samples by as much as 50 per cent at 10,000 psig. Wyble (1958) performed similar experiments on three different sandstone samples to determine the changes in conductivity, porosity and permeability at pressure range 0 to 5,000 psig. His results were consistent with the observation by Fatt and Davis (1952). During the experiments, different overburden pressures (radial force) were applied only to the cylinder core while the axial direction was kept at constant atmospheric pressure.

Gray *et al.* (1963) enhanced the previous experiments by applying axial force and combining with overburden pressure (radial force) to measure the anisotropy permeability changes at more representative reservoir stress-state condition. They showed that permeability reduction subjected to overburden pressure as a function of the ratio of radial to axial stress and the permeability reduction under non-uniform stress (radial pressure  $\neq$  axial pressure) is less than that under uniform stress.

Although extensive work has been established on the effect of overburden pressure and stress-state on matrix permeability but there are some very interesting details of fractured rock behavior under stress that have not been investigated.

In this study we will show the effect of fracture aperture and fracture permeability on the fluid flow under different overburden pressure. This study is a precursor to investigating fracture apertures under different stress-state conditions (confining stress, hydrostatic stress and triaxial stress) and imaging fracture aperture distributions using X-ray CT.

## **Experimental Work**

For simplicity and the difficulty of applying force in the axial direction, these experiments assume the axial direction is in the atmospheric pressure. Thus, only overburden pressure generated from hydraulic jack was applied to cylindrical core faces. Synthetic brine was used in the experiments. The brine contains NaCl and CaCl<sub>2</sub>. H<sub>2</sub>O mixed with distilled water. The clean core was saturated with brine then it was inserted into a Hassler-type core holder using a confining pressure of 500 psia. Then, core flooding was performed with different injection rates. After running set of injection rates at this pressure, we changed to other confining pressures and performed with different injection rates again. Similar procedure was performed using fractured core. Details of procedure for conducting core flooding experiments can be found in Appendix-A. The

procedure can be used for single and two phases experiments. The current results are mostly from the single-phase experiments. Even though one experiment has been done using two-phase flow, water and kerosene, but the result is not included in our discussion. The experiment set up (Fig. 1) is used for future experiments in which the kerosene will be replaced with the oil to investigate the fluid interaction through matrix and fracture or vice versa.

A Berea core was used during the core flooding experiments. The core properties are given in the note remark of Table 1. Two sets of injection rates ranging from 5 cc/min to 20 cc/min were performed at each overburden pressure. Three different overburden pressures were applied started from 500 to 1500 psia as listed in Tables 1 and 2 for both unfractured and fractured Berea core. The core was cut using a hydraulic cutter to generate fracture horizontally along the axis of the core. During the experiments using a fractured core, the pressure drop across the core is lower and the core permeability increases about 3 times higher compared to those obtained using unfractured core.

Figure 2 shows that the effect of varying overburden pressures on unfractured core is not significant in contrast with that effect on fractured core. The average permeability of fractured core significantly reduces and even reaches toward the permeability of unfractured core at 1500 psia. The pressure drops across unfractured core are parallel to the increase in injection rates therefore the permeability remains constant. Meanwhile, an increase in pressure drop causes large changes in average permeability of fractured core as depicted by Fig. 3. The result suggests that the effect of stresses may be most pronounced in fractured reservoirs where large pressure changes can cause significant changes in fracture aperture and the related changes in conductivity within a reservoir as also mentioned by Lorenz (1999).

## Data Analysis

In order to properly quantify the effect of fracture permeability on the fluid flow, it is important to describe the equations describing the changes of this parameter under different overburden pressure. The equations governing the fluid flow through fractures have been widely published in the reservoir engineering literature and are not discussed here. However, the pertinent equations used for our analysis are presented as follows:

The fracture permeability,  $k_f$ , is obtained by combining the viscous force and Darcy equation for flow through fractures as given below,

$$k_f = 8.45 \times 10^9 w^2 \dots\dots\dots(1)$$

where  $w$  is a fracture width in centimeters.

Fracture width is a function of fracture permeability and those two parameters are unknown. To obtain those parameters, one more equation is needed.

We obtained the average permeability of fracture and matrix,  $k_{av}$ , from core flooding experiments using a fractured core and matrix permeability,  $k_m$ , using unfractured core.

Thus, another fracture permeability equation can be obtained following this equation below.

$$k_f = \frac{k_{av}A - k_m(A - wl)}{wl} \dots\dots\dots(2)$$

where  $A$  is matrix area (cm<sup>2</sup>) and  $l$  is diameter of the core (cm).

Now, we have two equations and two unknowns. So, combining equations 1 and 2 can solve the fracture permeability and fracture width. First, the equation 3 is applied to solve  $w$  then it is inserted to equation 1 to solve  $k_f$ .

$$8.45 \times 10^9 w^3 l - k_{av}A + k_m(A - wl) = 0 \dots\dots\dots(3)$$

It is also important to determine the contribution flow rate from the matrix ( $q_m$ ) and fracture ( $q_f$ ). We determine the contribution from each zone by applying Darcy's equations. The equation for flow rate in matrix is:

$$q_m = \frac{k_m A \Delta p}{\mu L} \dots\dots\dots(4)$$

where  $q_m$  is the matrix flow rate (cc/sec),  $k_m$  is the matrix permeability (Darcy),  $A$  is the matrix area (cm<sup>2</sup>),  $\Delta p$  is pressure drop across the core (atm),  $\mu$  is viscosity (cp) and  $L$  is core length (cm).

The flow through a smooth conduit can be expressed by involving the fracture width ( $w$ ) and the pressure gradient ( $\Delta p$ ):

$$q_f = 9.86 \times 10^{-9} \frac{w^3 l \Delta p}{12 \mu L} \dots\dots\dots(5)$$

where  $q_f$  is the fracture flow rate (cc/sec),  $w$  is the fracture width (cm),  $l$  is a lateral extend of the fracture (cm),  $\Delta p$  is pressure drop across the core (atm),  $\mu$  is viscosity (cp) and  $L$  is core length (cm).

### Artificially Fractured Core Simulation

A numerical model utilizing commercial simulator (CMG™) was used to study the fluid flow through fracture at different overburden pressures. The laboratory process in which the water was injected through the fracture was duplicated in this modeling effort. The rectangular grid block was applied to overcome the difficulty of modeling a cylindrical core shape (Putra *et al.* [1999]). A 31x31 grid blocks were used in the x and z directions with 1 grid block in the y direction. The fracture layer is located only in the 16th layer and the rest are matrix layers. The permeability in fracture layer was calculated based on

two parallel plates without fracture roughness. All the layers were injected with constant water injection of 5 cc/hr. At the opposite end, two production points were located in the matrix and fracture layers to quantify the amount of water produced at those two points.

In the experimental process, the core is saturated with the water. Once water injection was started with constant rate, water was produced simultaneously. Then the water that was produced from both matrix and fracture layers at the end point was recorded. In the simulation, however, the initial water saturation condition is assumed zero. Thus, the water saturation change in the matrix and fracture can be observed as illustrated in Fig. 4. A few minutes after the injection was started, the flow rate was still in the transient condition and then reached a steady state condition at later time as shown in Fig. 5. At steady state condition, we recorded the amount of water produced from matrix and fracture. Similar simulation runs were performed for different overburden pressures. The results were compared with the experimental results as shown in Figs. 6 and 7. The dotted lines indicate the experimental results. Even though the quality of the match for both flow rate and pressure drop are not quite good due to using a single fracture model, which assumed smooth fracture surface between two parallel plates but the simulation results follows the trend of the laboratory results. To obtain a better result, we will extend our research by introducing the fracture aperture heterogeneity along each flow path.

## Results and Discussion

The fracture aperture and fracture permeability are usually considered to remain the same during the producing life of the reservoir regardless of degree of depletion. Our experimental results show that the fracture aperture and fracture permeability have significant pressure-dependent changes in response to applying variable injection rates and overburden pressures.

Figures 8 to 10 shows the effect of several injection rates on matrix permeability, fracture aperture and fracture permeability, respectively, under variable overburden pressures. The effect of several injections on matrix permeability is not significant in contrast with that effect on fracture aperture and fracture permeability. During constant injection rates of 5 to 20 cc/min, the average matrix permeability decreases about 24% at overburden pressure of 1500 psia from its original value at 500 psia. Meanwhile, the average fracture aperture and fracture permeability decrease about 71% and 91%, respectively, from its original value.

A very different behavior of the curve is observed for the first injection rate compared to the other injection rates. After the first injection rate at 500 psia, the fracture aperture at injection rates of 10, 15 and 20 cc/min has similar values. Meanwhile after increasing the overburden pressure, the effect of injection rates on fracture aperture is more obvious. As overburden pressure increases the higher injection rates the more reduction in fracture aperture. The fracture aperture becomes smaller at higher injection rates, which is the *opposite* with the common thought. The reason behind this phenomenon is because the core has high matrix permeability and surrounded by constant high confining pressure that does not allow core to expanding. The amount of flow at different injection rates

through the fracture drops dramatically and they almost flow at similar rate at confining pressure of 1500 psia (about 1 cc/min) as shown in Fig. 11. It means that the water mostly flows through the matrix diverting from the fracture path. At higher injection rates, the pressure drop becomes higher through the matrix and increases tendency to squeeze the fracture aperture. That is why the fracture aperture becomes smaller at higher injection rates.

The results also indicate that the influence of high stress on axial direction by introducing high injection rates would give high permeability reduction as also previous reported by Gray *et al.* (1963).

Because the fracture width is a function of fracture permeability, thus, the fracture permeability has similar trend as fracture width under different overburden pressures. The fracture permeability ranges from about 200-700 darcys at 500 psia reduces to about 9-36 darcys at 1500 psia.

We also calculated the reduction of matrix porosity to investigate the magnitude of rock compaction with adopting the following equation (Jin *et al.*, [2000]):

$$\frac{k}{k_o} = \left(\frac{\phi}{\phi_o}\right)^3 \dots\dots\dots(6)$$

where n=3 which is commonly used, corresponds to representation of porous space as an ensemble of flat channels and n=10 is used for real sandstones. The change in porosity with different overburden pressure has shown to be small compared to significant effect on permeability. The average matrix porosity change in different overburden pressure is only 3% compared to 24% change in matrix permeability.

The effect of reduction fracture permeability clearly has significant effect on reservoir productivity. Thus, we determine how much the reduction of fluid flow through the fracture because of reduction in fracture permeability. It is also important to quantify of the flow through the matrix and the fracture at different overburden pressures. By applying Equations 4 and 5, we were able to quantify the contribution of fluid flow from matrix and fracture as shown in Figs. 11 and 12 at variable overburden pressures. At 500 psia, the flow is preference to the high permeability zone. In this time, the percentage range of fluid flows through the fracture at injection range of 5 to 20 cc/min is 72% to 68%. Meanwhile, after increasing the overburden pressure the fluid flows through the fracture decreases. At 1500 psia, the percentage range of fluid flows through the fracture at different injection rate is only 14% to 2%. At this time most of injected water diverts through the matrix because of significant reduction of permeability in the fracture.

Even though the fracture permeability is still very high (10 to 40 darcys) but the volumetric rate of fracture becomes limited, therefore, most of the water flows through the matrix rock with having less permeability (>200 md) but higher volumetric rate.

## Conclusions

1. The laboratory result shows that the change in overburden pressure significantly affects the reservoir properties.
2. The change in matrix permeability with different injection rates under variable overburden pressures is not significant in contrast with that effect on fracture aperture and fracture permeability.
3. The experimental results of a core-induced fracture with high permeability matrix reveal that higher injection rates give smaller fracture aperture at constant high confining pressure.
4. The simulation results suggest that a parallel model is insufficient to predict fluid flow in the fracture system. Consequently, the spatial heterogeneity in the fracture aperture must be included in the modeling of fluid flow through fracture system.
5. The results also infer that the effect of stresses may be most pronounced in fractured reservoirs where large pressure changes can cause significant changes in fracture aperture and related changes in fractured permeability.
6. The change in porosity with different overburden pressure has shown to be small compared to significant effect on permeability.
7. At high overburden pressure the influence of existing fracture permeability on fluid flow contributor in permeable rocks ( $> 200$  md) is not too significant.

## References

1. Fatt, I. and Davis, D.H.: "Reduction in Permeability with Overburden Pressure," *Trans.*, AIME (1952) **195**, 329.
2. Gray H. D., Fatt, I., and Bergamini, G.: "The Effect of Stress on Permeability of Sandstone Cores," *SPEJ* (June 1963).
3. Jin, M., Somerville, J. and Smart, B.G.D.: "Coupled Reservoir Simulation Applied to the Management of Production Induced Stress-Sensitivity," paper SPE 64790 presented at the 2000 International Oil and Gas Conference and Exhibition, Cina, Nov 7-10.
4. Lorenz, J.C.: "Stress-Sensitive Reservoirs," *JPT* (Jan 1999), 61.
5. Putra, E., Fidra, Y., and Schechter, D.S.: "Study of Waterflooding Process in Naturally Fractured Reservoirs from Static and Dynamic Imbibition Experiments," paper SCA 9910 presented at the 1999 International Symposium of the Society of Core Analysts, Colorado, August 1-4.
6. Wyble, D.O.: "Effect of Applied Pressure on the Conductivity, Porosity and Permeability on Sandstones," *Trans.*, AIME (1958) **213**, 430.

## Nomenclatures

- $A$  = matrix area ( $\text{cm}^2$ )  
 $k_m$  = the matrix permeability (Darcy)  
 $k_f$  = the fracture permeability (Darcy)  
 $L$  = core length (cm)

$l$  = diameter of the core (cm)  
 $q_m$  = the matrix flow rate (cc/sec)  
 $q_f$  = the fracture flow rate (cc/sec)  
 $w$  = the fracture width (cm)  
 $\Delta p$  = pressure drop across the core (atm)  
 $\mu$  = viscosity (cp)

## **Appendix A – Procedure for Conducting Core Flooding Experiment**

### **For single phase experiments:**

1. Wash the core before saturating the core at about 350°C temperature for about two days.
2. Saturate the core before starting the experiment for about two days.
3. Make sure the two valves between the pumps and the accumulators are turned off before refilling the pumps.
4. Obtain the desired overburden pressure using hydraulic jack. This may cause several attempts to stabilize, as there will be air trapped in line causing you to lose overburden pressure.
5. Fill brine in accumulator 1 and kerosene or oil in accumulator 2, if necessary.
6. Turn on the valve between the pump 1 and the accumulator 1, and turn the valves to on position on the permeameter.
7. Turn the red valve to on position, which connects accumulator 1 to the core holder. Make sure that the black valve connecting accumulator 2 and core holder is off.
8. Perform the core flooding experiment with different flow rates and note the pressure difference in the permeameter.
9. Change the overburden pressure and perform the experiment and note the readings.
10. Fracture the core and place it again in the core holder and apply overburden pressure. Close the black valve and open the red valve again and perform the core flooding experiment with brine. Note the readings.

### **For two phase experiments:**

Follow until 9<sup>th</sup> procedures and continue with the following:

1. Turn the red valve to off position and open the valve between pump 2 and accumulator 2.
2. Also open the black valve that connects accumulator 2 to core holder.
3. Perform the core flooding experiment.
4. Note the amount of brine coming out of the core when kerosene or oil is injected.
5. Fracture the core and place it again in the core holder and apply overburden pressure. Close the black valve and open the red valve again and perform the core flooding experiment with brine.
6. Note the amount of kerosene or oil discharged when brine is injected.

## **Precautions**

1. Filter the brine to avoid any dissolved solids that choke the core.
2. Make sure the experiment is performed without any air trapped in the core.
3. While refilling the accumulators, care should be taken to close the valves between accumulator and core holder to avoid any air entering the pipelines.
4. Fracture the core as soon as possible to avoid much loss of fluid.
5. Note the volume of outlet pipeline from the core holder and subtract it from the amount of brine discharged while kerosene is injected.
6. After each flow, allow the pressure to drop close to atmospheric pressure before starting the next flow.

Table –1 Overburden experiments for unfactured core.

<b>Pob psia</b>	<b>Dp psia</b>	<b>k<sub>m</sub> md</b>	<b>Q Cm<sup>3</sup>/m</b>
485.7	4.1	299.7	5
506.4	8.1	303.4	10
502.9	12.4	297.2	15
504.4	16.5	297.85	20
501	4.2	292.5	5
504.9	8.5	289	10
501	13	283	15
502	17	289.1	20
1000.4	4.5	273	5
1002.4	9	273	10
1000.5	13.7	269	15
1000.5	18.2	270	20
1000.2	4.8	255.9	5
1003.5	9.7	253.3	10
1002.7	14.5	254.2	15
1004.1	19.2	255.96	20
1500	5.1	240.8	5
1500	10.4	236.3	10
1500.7	16.4	224.7	15
1503.1	22.1	222.4	20
1500.3	5.5	223.4	5
1501	11.2	219.4	10
1501.3	17.3	213	15
1502.3	22.7	216.5	20

Table –2 Overburden experiments for fractured core.

<b>Pob psia</b>	<b>Dp psia</b>	<b>k<sub>av</sub> md</b>	<b>Q Cm<sup>3</sup>/m</b>
501.3	1.4	877.5	5
500.2	2.8	877.6	10
503.3	4.1	898.9	15
503.3	5.4	910	20
494.8	1	1228.7	5
509.4	2.6	945.1	10
508.8	4.2	877.6	15
509.6	5.8	847.3	20
970.5	2.2	558.4	5
1000.5	4.8	511.9	10
1001	7.6	485	15
1016.7	11.3	434.9	20
1000.8	2.3	534	5
1002.2	5.8	423.6	10
1009.7	9.1	405	15
1002.7	13.9	353.6	20
1500.3	4.2	292.5	5
1504.6	9.3	268.2	10
1507.9	15.1	244.1	15
1504.8	21.4	229.6	20
1500.7	5	245.7	5
1506	10.9	225.4	10
1509.6	17.4	211.8	15
1509.6	22.5	218.4	20

NOTE:

**Berea Core Properties**

Length           4.9784 Cm  
Diameter        2.5146 Cm  
Viscosity        1.0 Cp  
Area             4.9637 Cm<sup>2</sup>  
Porosity         23.58%

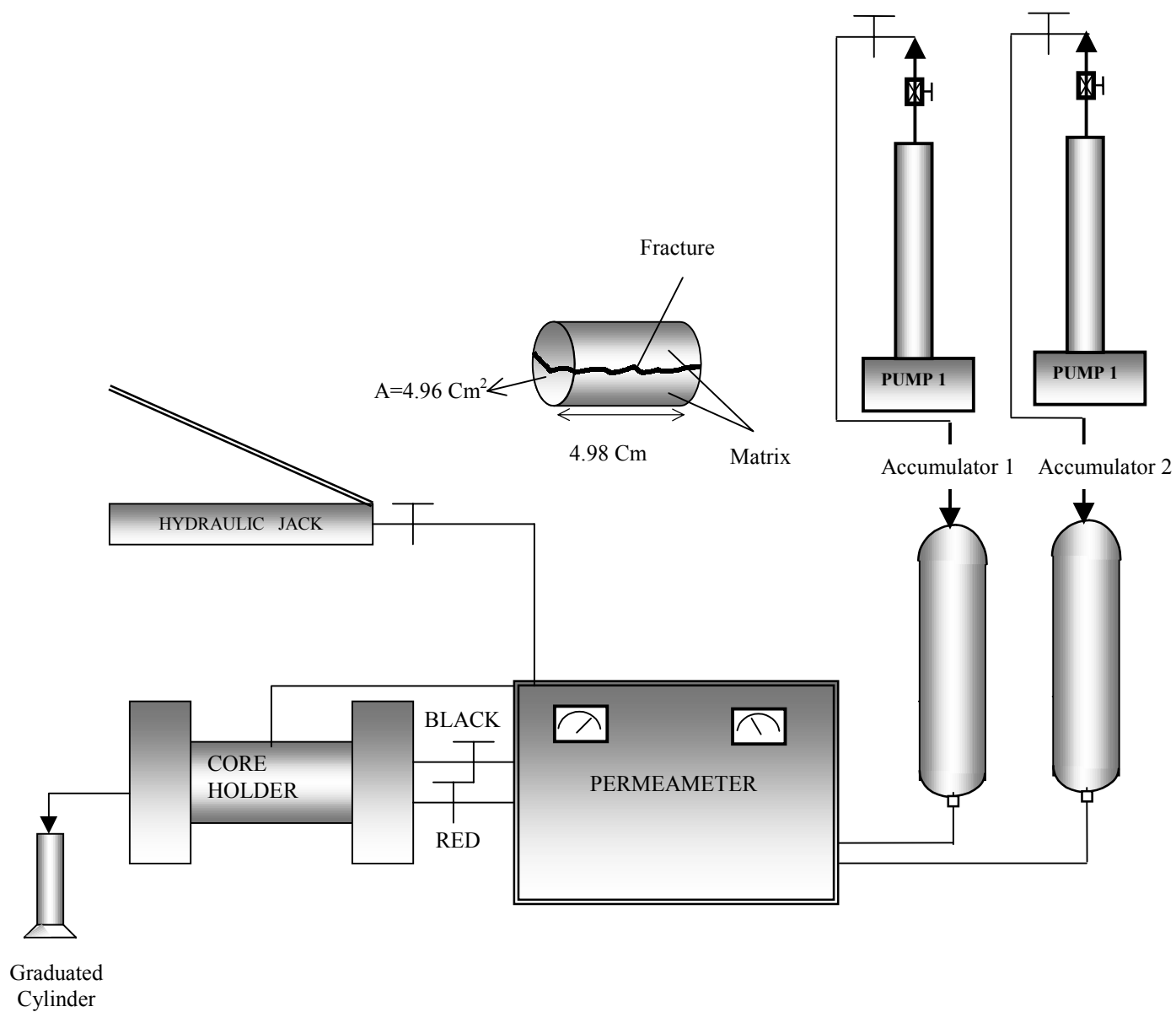


Fig. 1 - Schematic diagram of the two-phase core flooding experiment.

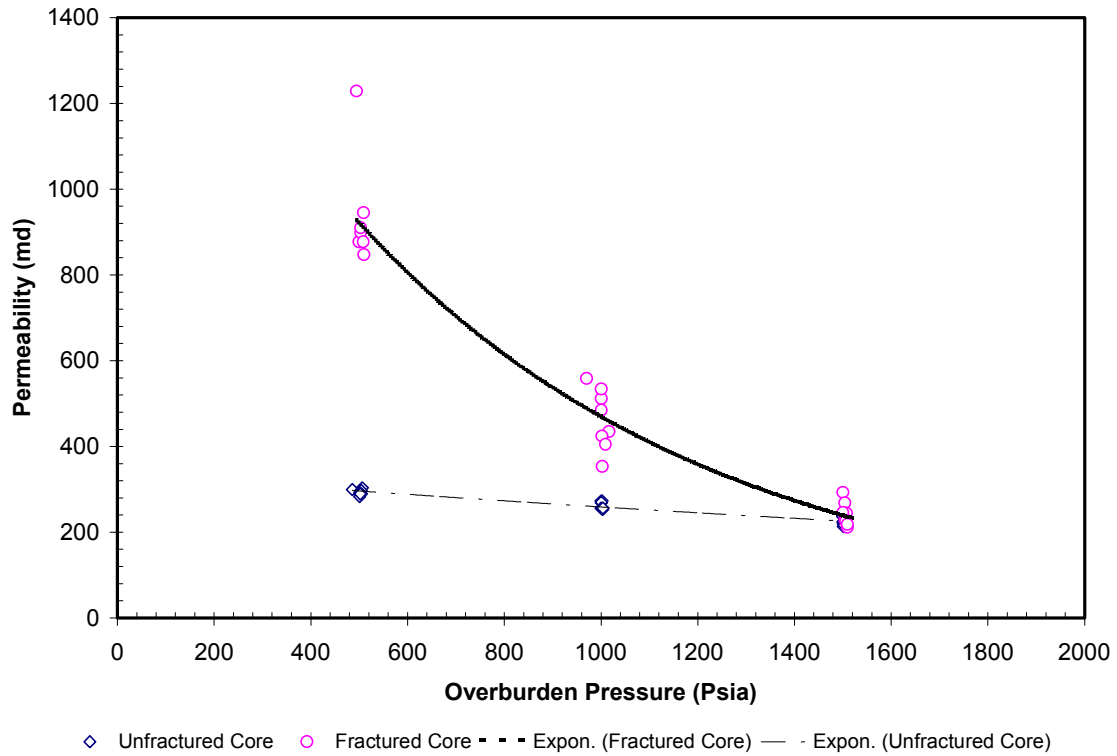


Fig. 2 – Comparison permeability reduction between unfractured and fractured cores due to increasing overburden pressure.

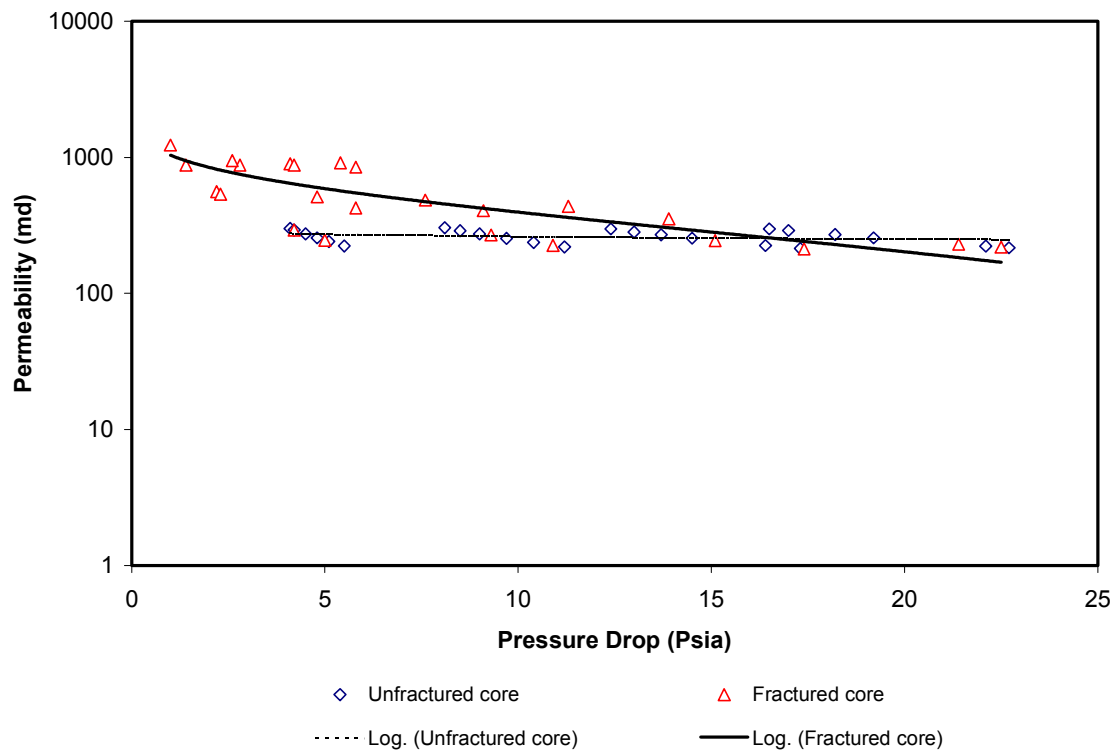


Fig. 3 –Relationship between pressure drop and permeability.

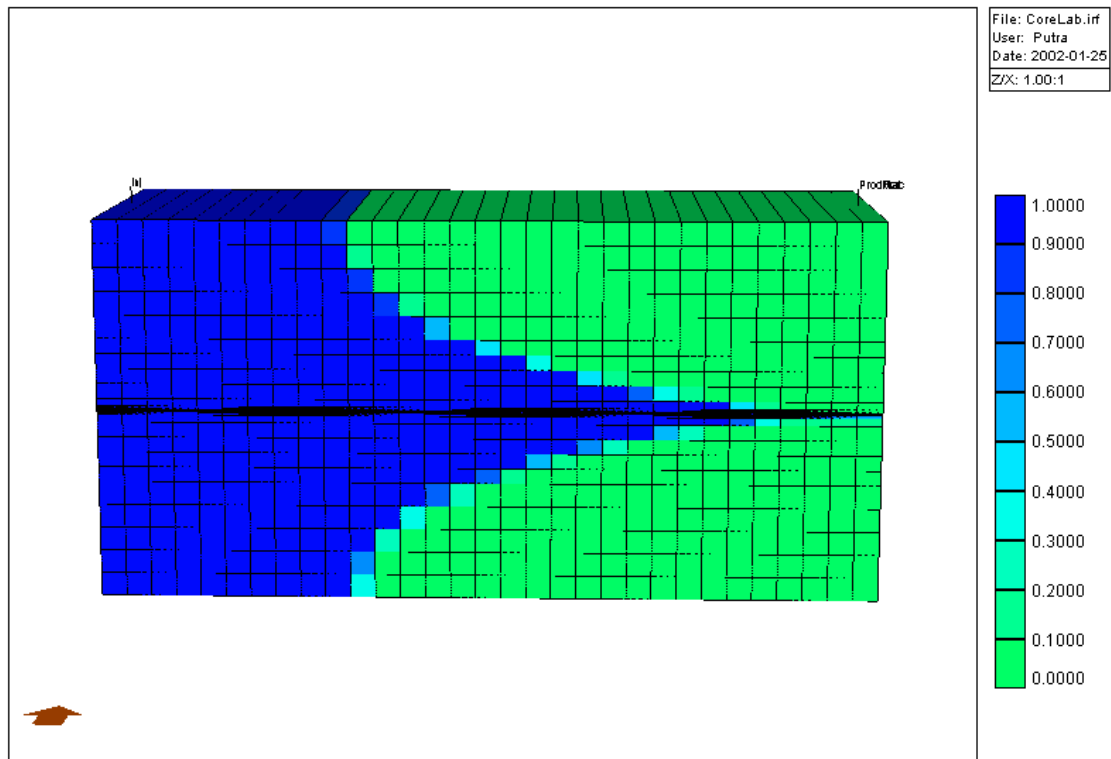


Fig. 4 - Water saturation change at matrix and fracture at transient flow condition.

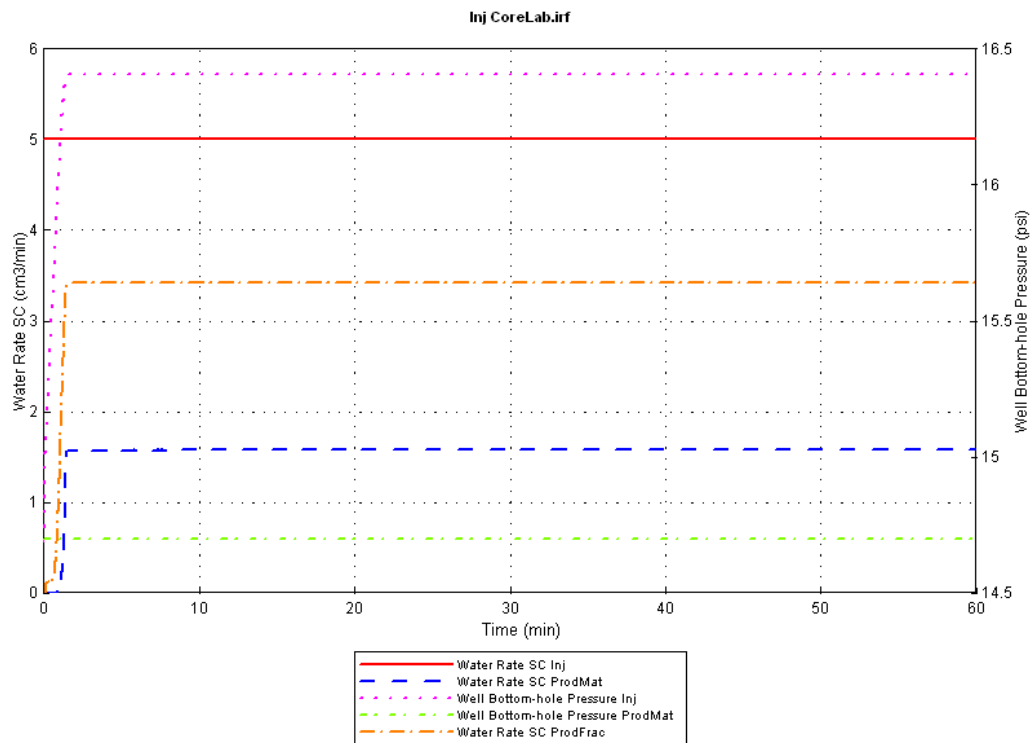


Fig. 5 – The simulation results of flow rates and pressure drop injected at 5 cc/min and overburden pressure of 500 psi.

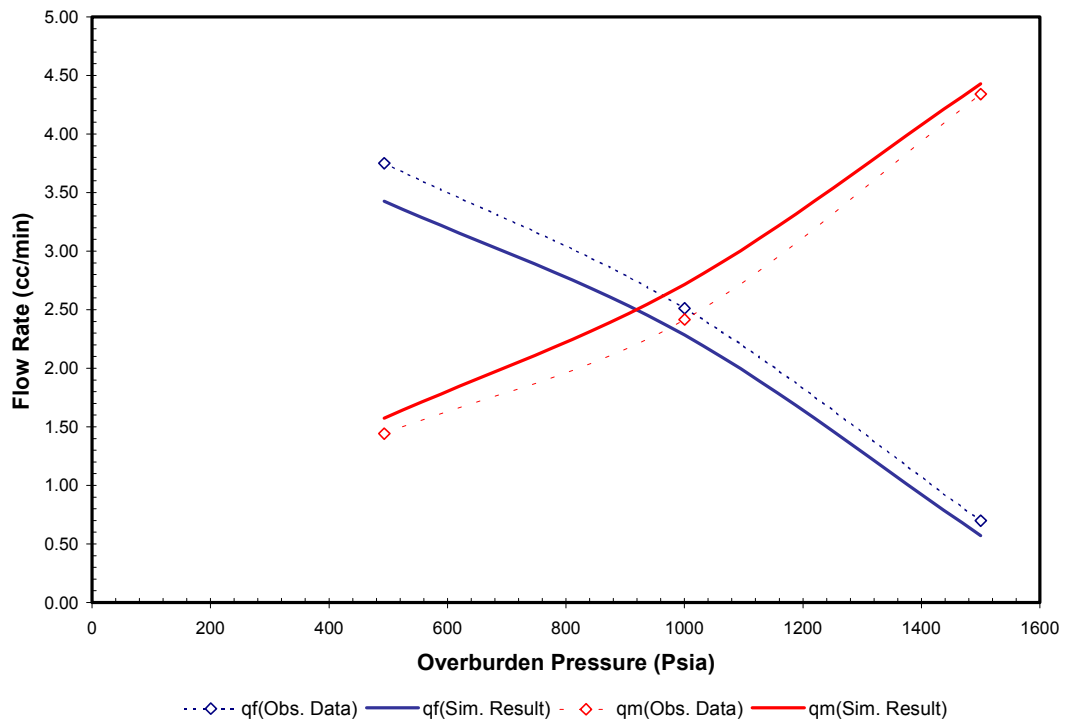


Fig. 6 – The flow rates comparison between laboratory and simulation results at 5 cc/min and each different overburden pressures.

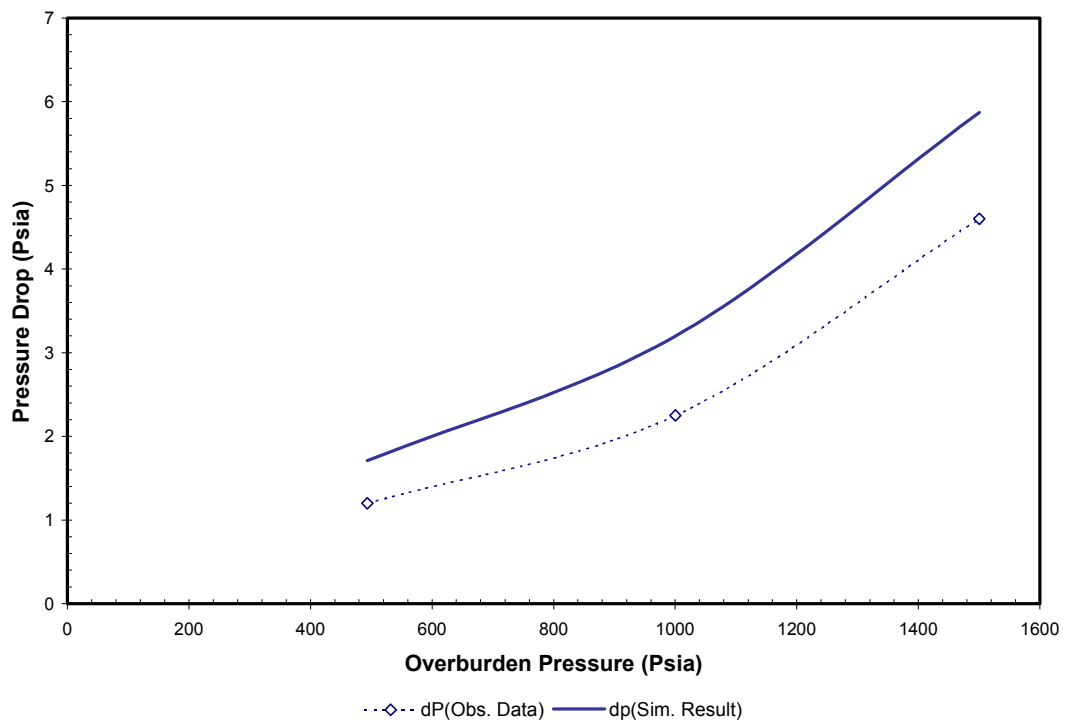


Fig. 7 – The pressure drop comparison between laboratory and simulation results at 5 cc/min and each different overburden pressures.

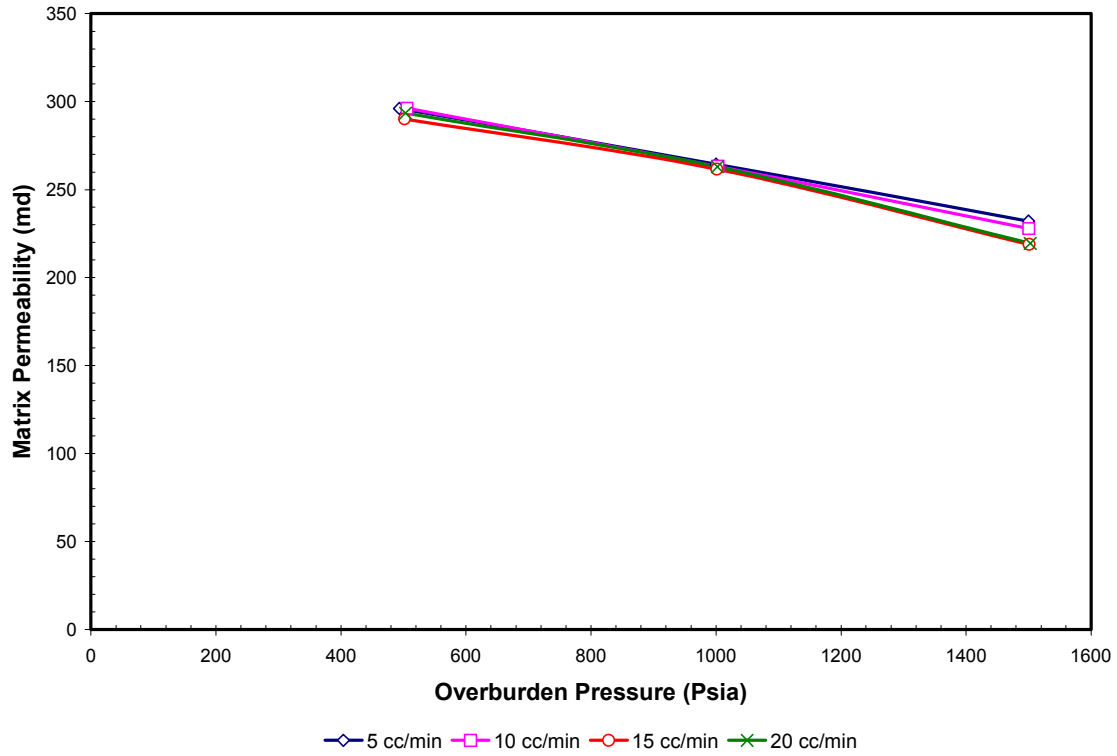


Fig. 8 –Effect of injection rates on matrix permeability during applying variable overburden pressures.

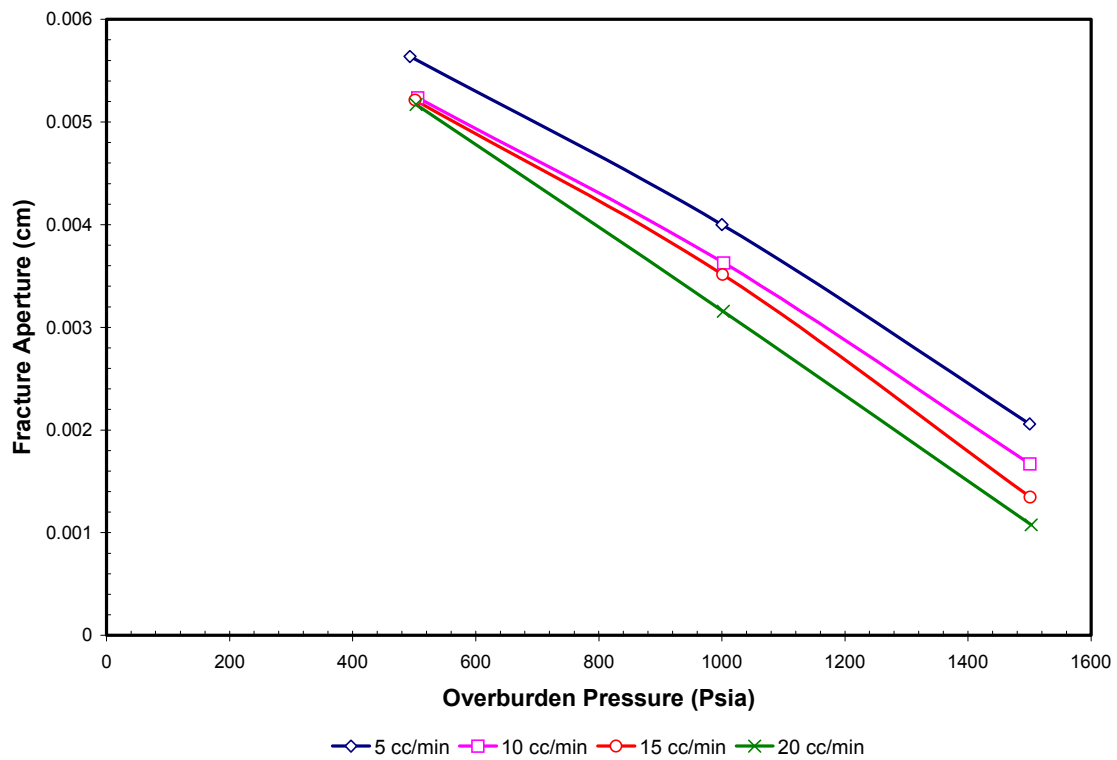


Fig. 9 – Effect of injection rates on fracture aperture during applying variable overburden pressures.

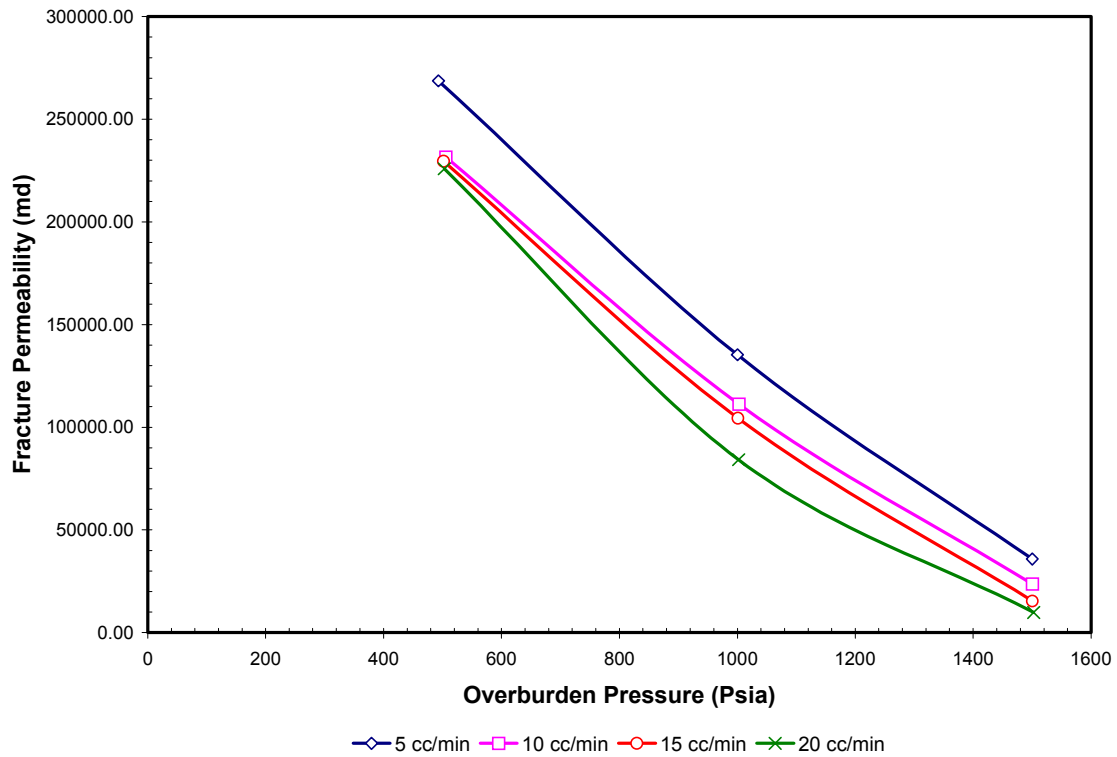


Fig. 10 –Effect of injection rates on fracture permeability during applying variable overburden pressure.

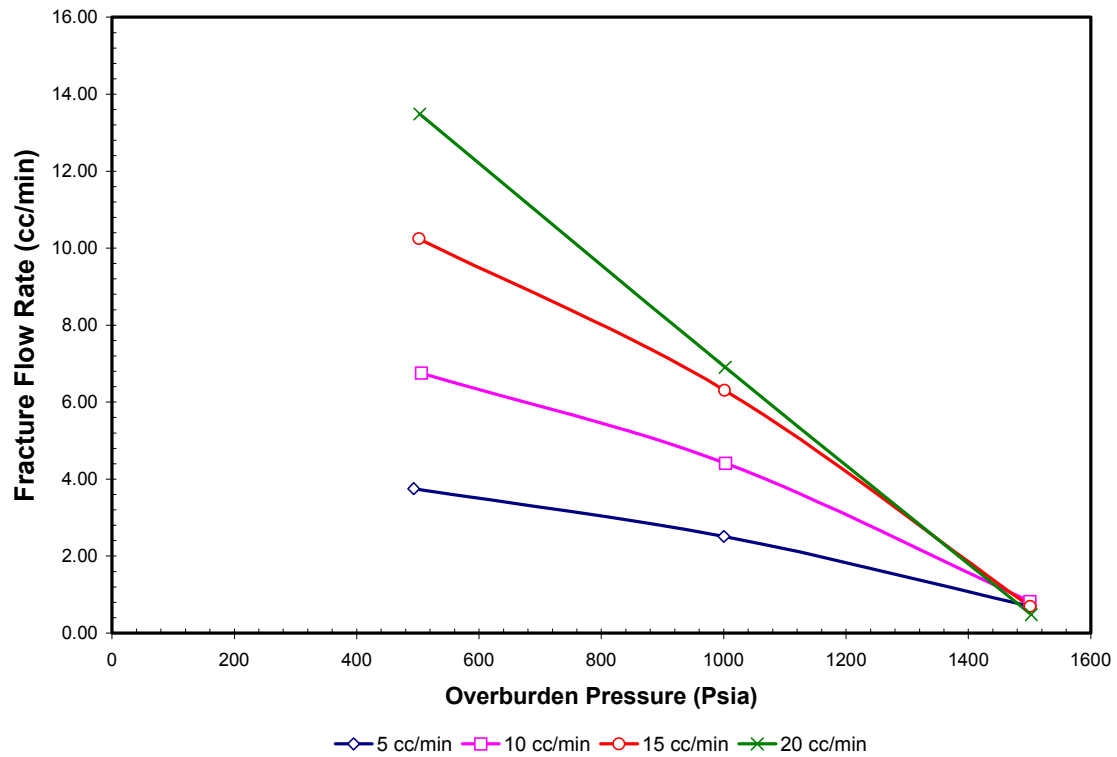


Fig. 11 – Reduction in fracture flow rate during variable overburden pressures.

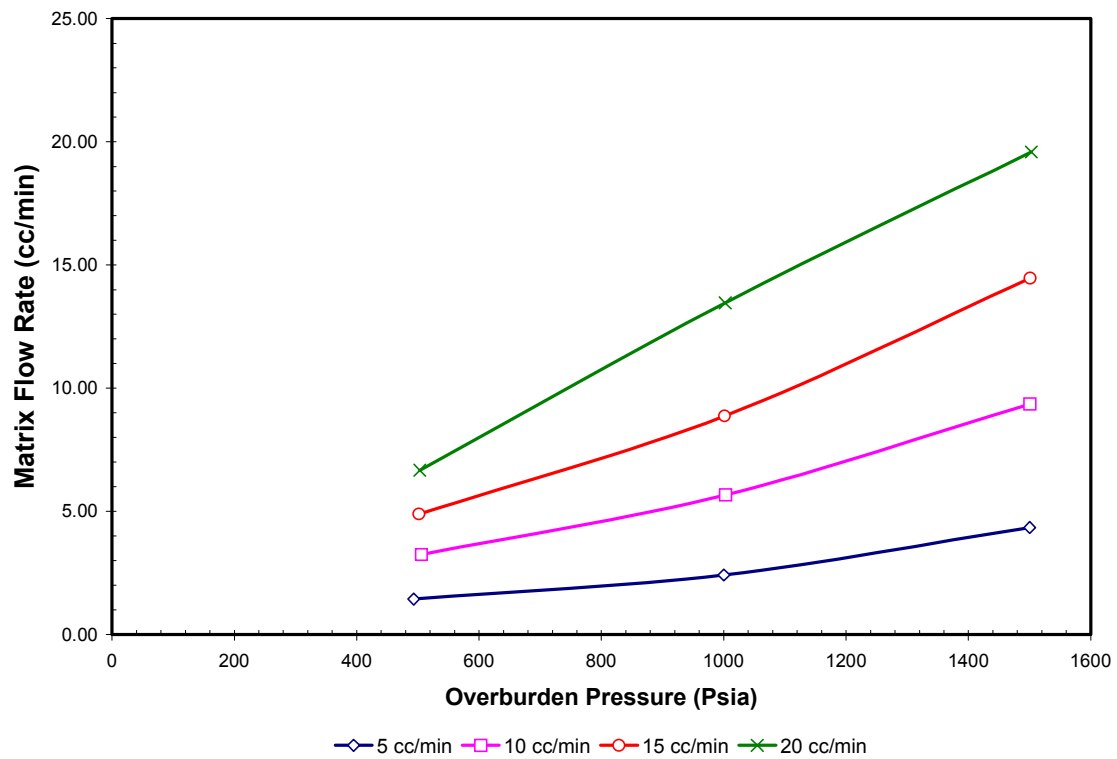


Fig. 12 – Reduction in matrix flow rate during variable overburden pressures.